

Amyloid PET predicts atrophy in older adults without dementia: Results from the AMYPAD Prognostic & Natural History study

Leonard Pieperhoff ^{a,b,1,*}, Luigi Lorenzini ^{a,b,1}, Sophie Mastenbroek ^{a,b,c},
 Mario Tranfa ^{a,b,d}, Mahnaz Shekari ^{e,f}, Alle Meije Wink ^{a,b}, Robin Wolz ^g, Sylke Grootoont ^g,
 Craig Ritchie ^h, Mercè Boada ^{i,j}, Marta Marquié ^{i,j}, Wiesje van der Flier ^{b,k,l}, Rik Vandenberghe ^m,
 Bernard J. Hanseeuw ^{n,o}, Pablo Martínez-Lage ^p, Pierre Payoux ^q, Pieter Jelle Visser ^{b,k},
 Michael Schöll ^{r,s,t}, Giovanni B. Frisoni ^u, Andrew Stephens ^v, Christopher Buckley ^w,
 Gill Farrar ^w, Frank Jessen ^x, Oriol Grau-Rivera ^e, Juan Domingo Gispert ^e,
 David Vállez García ^{a,b,e}, Henk Mutsaerts ^{a,b}, Frederik Barkhof ^{a,b}, Lyduine E. Collij ^{a,b,c}, on
 behalf of the AMYPAD consortium

^a Department of Radiology and Nuclear Medicine, Vrije Universiteit Amsterdam, Amsterdam University Medical Center, Amsterdam 1081HV, the Netherlands

^b Amsterdam Neuroscience, Brain Imaging, Amsterdam 1081HV, the Netherlands

^c Clinical Memory Research Unit, Department of Clinical Sciences Malmö, Faculty of Medicine, Lund University, Lund 211 46, Sweden

^d Department of Advanced Biomedical Sciences, University "Federico II", Naples 80131, Italy

^e Barcelonaàguda Brain Research Center, Pasqual Maragall Foundation, Barcelona 08005, Spain

^f Hospital del Mar Medical Research Institute (IMIM), Barcelona 08003, Spain

^g IXICO, London EC1A 9PN, United Kingdom

^h Scottish Brain Sciences, Edinburgh EH12 9DQ Scotland, United Kingdom

ⁱ Ace Alzheimer Center Barcelona – Universitat Internacional de Catalunya, Barcelona 08014, Spain

^j Networking Research Center on Neurodegenerative Diseases (CIBERNED), Instituto de Salud Carlos III, Madrid 28031, Spain

^k Alzheimer Center Amsterdam, Neurology, Vrije Universiteit Amsterdam, Amsterdam University Medical Center, Amsterdam 1081HV, the Netherlands

^l Epidemiology and Data Science, Vrije Universiteit Amsterdam, Amsterdam UMC Location VUmc, Amsterdam 1081HV, the Netherlands

^m Katholieke Universiteit Leuven, Leuven 3000, Belgium

ⁿ Department of Neurology, Cliniques Universitaires Saint-Luc, Brussels 1200, Belgium

^o Institute of Neuroscience, Université catholique de Louvain, Brussels 1200, Belgium

^p Center for Research and Advanced Therapies, CITA Alzheimer Foundation, Donostia-San Sebastián, 20009, Spain

^q Université Toulouse 3, Inserm, ToNIC Toulouse NeuroImaging Center, Toulouse 31024, France

^r Department of Psychiatry and Neurochemistry, Institute of Neuroscience and Physiology, The Sahlgrenska Academy, University of Gothenburg, Gothenburg 413 45, Sweden

^s Wallenberg Centre for Molecular and Translational Medicine, University of Gothenburg, Gothenburg 411 26, Sweden

^t Dementia Research Centre, Institute of Neurology, University College London, London WC1N 3AR, United Kingdom

^u Hôpitaux Universitaires de Genève, Geneva 1205, Switzerland

^v Life Molecular Imaging, Berlin 13353, Germany

^w GE HealthCare, Buckinghamshire HP8 4SP, United Kingdom

^x Department of Psychiatry and Psychotherapy, University Hospital Cologne, Cologne 50937, Germany

ARTICLE INFO

ABSTRACT

Keywords:

Centiloid
 MRI
 Gray Matter Thickness
 Gray Matter Volume
 Preclinical Alzheimer's Disease
 Cognitively Unimpaired

The impact of amyloid- β (A β) accumulation on regional brain atrophy in preclinical Alzheimer's disease (AD), and its interaction with risk factors like sex and APOE- ϵ 4 carriership, remains unclear. In this study, we examined these associations in a population of older adults without dementia and evaluated the potential of A β -PET for risk stratification.

We included 1329 participants (56 % female) with an age of 68.2 ± 8.78 years from the prospective multi-center AMYPAD Prognostic and Natural History Study who underwent [^{18}F]Flutemetamol or [^{18}F]Florbetaben

* Corresponding author at: Amsterdam Universitair Medische Centra, de Boelelaan 1117, PK-1X014, Amsterdam 1081HV, the Netherlands.

E-mail address: l.pieperhoff@amsterdamumc.nl (L. Pieperhoff).

¹ These authors contributed equally to this work.

$\text{A}\beta$ -PET and T1-weighted MRI, with longitudinal data for 684 participants (median follow-up = 3.4 years). Linear mixed models assessed the effect of baseline $\text{A}\beta$ burden through the Centiloid approach on longitudinal changes in regional gray matter volume and thickness. Sensitivity analyses were performed in cognitively normal only (CDR = 0) individuals and while correcting for CSF p-tau181 and t-tau. A second model investigated the effects of sex or *APOE*- $\epsilon 4$ carriership.

Baseline global $\text{A}\beta$ was predictive of widespread atrophy in several brain regions, most strongly in the fusiform ($\beta_{\text{Volume}} = -0.006$, $\beta_{\text{Thickness}} = -0.009$), hippocampus ($\beta_{\text{Volume}} = -0.005$), posterior cingulate ($\beta_{\text{Volume}} = -0.006$), and precuneus ($\beta_{\text{Volume}} = -0.004$, $\beta_{\text{Thickness}} = -0.007$), also when investigating only in cognitively normal individuals. Only fusiform atrophy ($\beta_{\text{p-tau}} = -0.011$; $\beta_{\text{t-tau}} = -0.011$) remained predicted by $\text{A}\beta$ when correcting for p-tau181 or t-tau. Temporal atrophy was exacerbated in women, while frontal, lateral-temporal and hippocampal atrophy was exacerbated by carriership of at least one *APOE*- $\epsilon 4$ allele, with volumetric loss more sensitive to sex effects and thinning more sensitive to *APOE*- $\epsilon 4$ effects.

Our findings suggest that in older adults with mostly preserved cognition, baseline $\text{A}\beta$ -PET predicts future brain atrophy, with fusiform atrophy showing independence from tau pathology and $\text{A}\beta$ -dependent atrophy being exacerbated in region-dependent manners in females and *APOE*- $\epsilon 4$ carriers. Regional cortical volume and thickness may serve as sensitive markers for early $\text{A}\beta$ -related neurodegeneration and aid in stratifying risk in AD prevention trials.

1. Introduction

Brain atrophy is a key feature of neurodegenerative diseases and a common surrogate endpoint in Alzheimer's disease (AD) clinical trials (Schwarz et al., 2019). In its clinical stage, AD-associated atrophy and cognitive decline are closely linked to tau deposition (Bejanin et al., 2017). However, as the field of anti-amyloid therapy is shifting towards early intervention, there is a need to better understand the predictive value of early amyloid-beta ($\text{A}\beta$) accumulation on atrophy in the pre-clinical stages of the disease.

AD-associated atrophy has commonly been described first in medial-temporal areas, followed by more widespread involvement of the neocortex (Chételat et al., 2012; La Joie et al., 2020; Tosun et al., 2011). Evidence on the effect that early amyloid deposition exerts on regional atrophy are conflicting, however, with some highlighting frontoparietal rather than medial-temporal atrophy patterns (Martikainen et al., 2019; Mattsson et al., 2014), while others have reported no observed atrophy (Josephs et al., 2008) or even increased volumes (Chételat et al., 2010; Ingala et al., 2021). This conflicting evidence may be partially explained by the heterogeneity of the measures used to quantify atrophy, e.g. volume or thickness, and local, regional and global analyses as well as the investigated disease stages. In a recent study, CSF measures of amyloid-beta 42 were predictive of medial-temporal atrophy rates in individuals without dementia, suggesting that amyloid deposition may lead to atrophy independently of CSF p-tau (Cacciaglia et al., 2025). However, CSF shows an early plateau effect and is less effective in tracking the extent of amyloid pathology compared to amyloid positron emission tomography (PET), which can be substantial even in cognitively unimpaired individuals (Collij et al., 2021; Salvadó et al., 2019). Taken together, these results underscore the need to further characterize the possible relationship between PET measured cerebral amyloid deposition and neurodegenerative processes in the earliest stages of the disease, with the goal of informing early secondary or even primary prevention strategies.

In addition, the individual vulnerability to AD-related neurodegenerative processes due to demographic and genetic risk factors must be taken into account (Kepp et al., 2023). Previous findings regarding the effect of *APOE*- $\epsilon 4$ carriership have reported either increased volume loss in lateral-temporal and superior-frontal regions in a cohort of amyloid-positive subjects with mild cognitive impairment (MCI) (Sauty and Durrleman, 2023) or widespread cortical thinning in prodromal AD *APOE*- $\epsilon 4$ non-carriers compared to carriers (Mattsson et al., 2018). These discrepancies may have arisen from the isolated examination of gray matter volume and thickness, highlighting the necessity for concurrent analyses of these image-derived phenotypes (IDPs). Regarding sex differences, women show higher AD prevalence (Gustavsson et al., 2023) faster accumulation of cortical tau as measured with PET (Wisch et al.,

2021) and greater cortical atrophy (Sauty and Durrleman, 2023) compared to males in clinical stages. In contrast, women in preclinical cohorts show a delayed and slower atrophy rate despite greater tau burden (Buckley et al., 2019; Sauty and Durrleman, 2023) illustrating the complexity of this relationship. Hence, understanding the moderating effects of demographic and genetic risk factors on the association between $\text{A}\beta$ burden and subsequent atrophy is crucial for informing clinical practice and patient selection/stratification in clinical trials.

The current study aims to determine the influence of global cortical amyloid burden on regional brain atrophy. To this end, we examined regional changes in brain volume and thickness in a large cohort composed of older adults without dementia from the Amyloid Imaging to Prevent Alzheimer's Disease (AMYPAD) Prognostic Natural History Study (PNHS). We further investigated how the relationship between $\text{A}\beta$ and atrophy is influenced by sex and *APOE*- $\epsilon 4$ carriership, and the additive predictive value of utilizing longitudinal amyloid-PET data.

2. Materials and methods

2.1. Participants

Data for this study were drawn from the AMYPAD PNHS v202306 ($N = 1585$) (García, 2023). The AMYPAD PNHS (EudraCT: 2018-002277-22) is a multi-center cohort of non-demented participants to determine the value of amyloid PET in clinical- and research settings; the study design has been described in detail previously (Collij et al., 2022a; Lopes Alves et al., 2020). Briefly, eligibility criteria for inclusion in the AMYPAD PNHS were no history of dementia (clinical dementia rating (CDR) < 1), age above 50 years, and being able to undergo an amyloid-PET and MRI scan. The studies were reviewed and approved by Medical Ethical Committee of the University Medical Center Amsterdam, location VUmc and all local sites. The studies were conducted according to the principles of the Helsinki Declaration of 1975, as revised in 2008, and all human participants gave written informed consent. Median time difference between the MRI and PET acquisition was 50 days (IQR 99 days). A subset of 684 participants underwent at least one follow-up PET and MRI, at a median follow-up of 3.4 years (± 1.4 years) after baseline. None of the study participants participated in clinical trials of anti-amyloid therapy throughout the duration of the study.

2.2. $\text{A}\beta$ -PET acquisition and Quantification

PET scans were acquired 90–110 min p.i. of 185 MBq ($\pm 10\%$) for [^{18}F]Flutemetamol and 350 MBq ($\pm 20\%$) for [^{18}F]Florbetaben, consisting of 4 frames of 5 min according to the standard protocol for each tracer (Barthel et al., 2011; Curtis et al., 2015). Image analysis was

Table 1

Demographics and Clinical Characteristics at Baseline.

	Overall (n = 1,329) ^a	Low A β (n = 952) ^a	Intermediate A β (n = 117) ^a	Elevated A β (n = 260) ^a	<i>p</i>
Age, years	68.18 (8.78)	66.47 (8.21)	70.64 (8.30)	73.33 (8.80)	<0.001 ^b
Follow-Up, years	3.74 (1.87)	3.81 (1.88)	3.54 (1.91)	3.39 (1.75)	0.037 ^b
(Missing)	585	355	58	172	
Sex, Female	741 (56 %)	545 (57 %)	63 (54 %)	133 (51 %)	0.2 ^c
Education, years	14.56 (3.97)	14.71 (3.96)	14.47 (3.84)	14.05 (4.01)	0.075 ^b
CDR					<0.001 ^c
0 – Normal	1,070 (81 %)	833 (88 %)	90 (77 %)	147 (57 %)	
0.5 – Very mild	259 (19 %)	119 (13 %)	27 (23 %)	113 (43 %)	
CDR at Follow-Up					<0.001 ^d
0 – Normal	572 (88 %)	486 (92 %)	40 (78 %)	46 (68 %)	
0.5 – Very mild	76 (12 %)	45 (8 %)	11 (22 %)	20 (29 %)	
1 – Mild	2 (0 %)	0 (0 %)	0 (0 %)	2 (3 %)	
(Missing)	679	421	66	192	
MMSE	28.82 (1.54)	29.06 (1.27)	28.68 (1.52)	27.91 (2.08)	<0.001 ^b
(Missing)	108	61	8	39	
<i>APOE-e4</i> carriership (% carriers)	517 (40 %)	300 (32 %)	58 (51 %)	159 (66 %)	<0.001 ^c
(Missing)	40	17	3	20	
Amyloid PET, Centiloid	19.51 (32.33)	2.81 (8.37)	28.55 (6.05)	76.58 (27.48)	<0.001 ^b
est. Total Intracranial Volume, cm ^c	1477.71 (178.43)	1476.68 (177.60)	1477.94 (196.79)	1481.38 (173.41)	0.7 ^d

Abbreviations: A β , amyloid β ; CDR, Clinical Dementia Rating; MMSE, Mini-Mental State Examination; PET, Positron Emission Tomography; Amyloid stages are defined based on a Centiloid value of under 20 for low, over 40 for elevated A β and a subsequent intermediate A β between 20 and 40CL.

^a Mean (SD); n / N (%).

^b Kruskal-Wallis rank sum test.

^c Pearson's Chi-squared test.

^d Fisher's exact test.

performed centrally using IXICO's automated workflow. Briefly, PET frames were co-registered, averaged, and aligned to the corresponding MRI scan, which was parcellated using a subject-specific multi-atlas approach, i.e. the learning embeddings for atlas propagation (LEAP) parcellation procedure.(Wolz et al., 2010) SUVR images were obtained using LEAP parcellation masks using the whole cerebellum as a reference region in native space. In order to pool A β -PET data across sites, SUVR values were transformed to Centiloids (CL) using the standard Global Alzheimer's Association Interactive Network target region as a measure of global amyloid burden.(Klunk et al., 2015).

Participants were grouped in low (CL \leq 20), intermediate (20 $<$ CL \leq 40), and elevated (CL $>$ 40) A β stages, corresponding to cut-points in current early secondary prevention trials(Rafii et al., 2023) and based on derived cut-offs to define reliable worsening and detection of amyloid plaques on neuropathology.(Jack et al., 2017; Villeneuve et al., 2015).

2.3. MRI acquisition and Quantification

3D T1-weighted MR images were acquired on Philips (n = 1340), Siemens (n = 761) or GE HealthCare (n = 24) scanners, all of which had a field strength of 3 T. All longitudinal MRI were acquired on the same scanner model. Cortical segmentation was performed with FreeSurfer v7.1.1 (surfer.nmr.mgh.harvard.edu/), including motion correction, skull-stripping, brain parcellation and estimation of regional gray matter volume and thickness. The details of these procedures are described elsewhere.(Reuter et al., 2012) The final IDPs included estimated total intracranial volume (eTIV), volumes of six sub- and allocortical regions of interest encompassing the lateral ventricles, thalamus, caudate, putamen, hippocampus and amygdala, as well as volume and thickness of 34 bilateral cortical regions of interest covering the whole cerebral cortex defined using the Desikan-Killiany atlas.(Desikan et al., 2006) The parcellations were visually quality controlled following an adapted version (Bocancea et al., 2023) of a previously published protocol including assessment of regional boundaries (Raamana et al., 2022), resulting in the exclusion of 36 subjects due to segmentation errors; minor boundary misalignments were not manually corrected (McCarthy et al., 2015; Vahermaa et al., 2023). IDPs were harmonized using neuroCombat v1.0.13 to remove batch effects, while preserving the

biological effects of age, sex and global CDR scores (Supplementary Fig. 1).(Fortin et al., 2018) Median follow-up time was 3.40 years (\pm 1.4 years) with a median of one follow-up visit.

2.4. Statistical analysis

All analyses were carried out in R v4.3.0 (www.r-project.org/). Differences in demographics between A β groups were assessed using ANOVA and Chi-Square tests for continuous- and categorical variables, respectively.

To assess the effect of baseline global cortical A β burden on subsequent regional neurodegeneration, linear mixed-effects models (LME) implemented via the R package "lme4" v1.1-35.3 with random slope and intercept were used. The main predictors included baseline amyloid burden (continuous CL), follow-up time, and their interaction while correcting for age and CDR at baseline, sex, *APOE-e4* status, years of education and eTIV; in R equation format: "GM Volume/Thickness ~ 1 + Centiloid_{Baseline} + Time + Centiloid_{Baseline}:Time + *APOE-e4* status + Years of Education + Age_{Baseline} + Sex + eTIV + CDR_{Baseline} + (1 + Time | Subject)".(Dhamala et al., 2022). As a sensitivity analysis, these analyses were repeated in the CDR = 0 subset (N = 1099).

To investigate whether baseline amyloid is predictive of atrophy independently of baseline CSF p-tau181 and t-tau levels, analyses were repeated in a subset of participants with available CSF biomarkers (N = 428; N = 808 visits). First, the same base model was run, followed by including baseline t-tau or baseline p-tau181 as an additional covariate.

To assess the added value of longitudinal A β -PET measurements in predicting subsequent atrophy, we also repeated the main analyses in the subset of participants with longitudinal PET (N = 684), in which we utilized time-varying Centiloid rather than baseline Centiloid. Cross-sectional-only (using baseline Centiloid) and longitudinal model fits were compared using the Akaike Information Criterion derived from ANOVA.

Finally, the effect of *APOE-e4* carriership and sex on amyloid-atrophy relationships was assessed using one additional LME model with two added three-way interactions, namely amyloid*time**APOE* and amyloid*time*sex.

All IDPs and CL values were z-scaled to obtain standardized

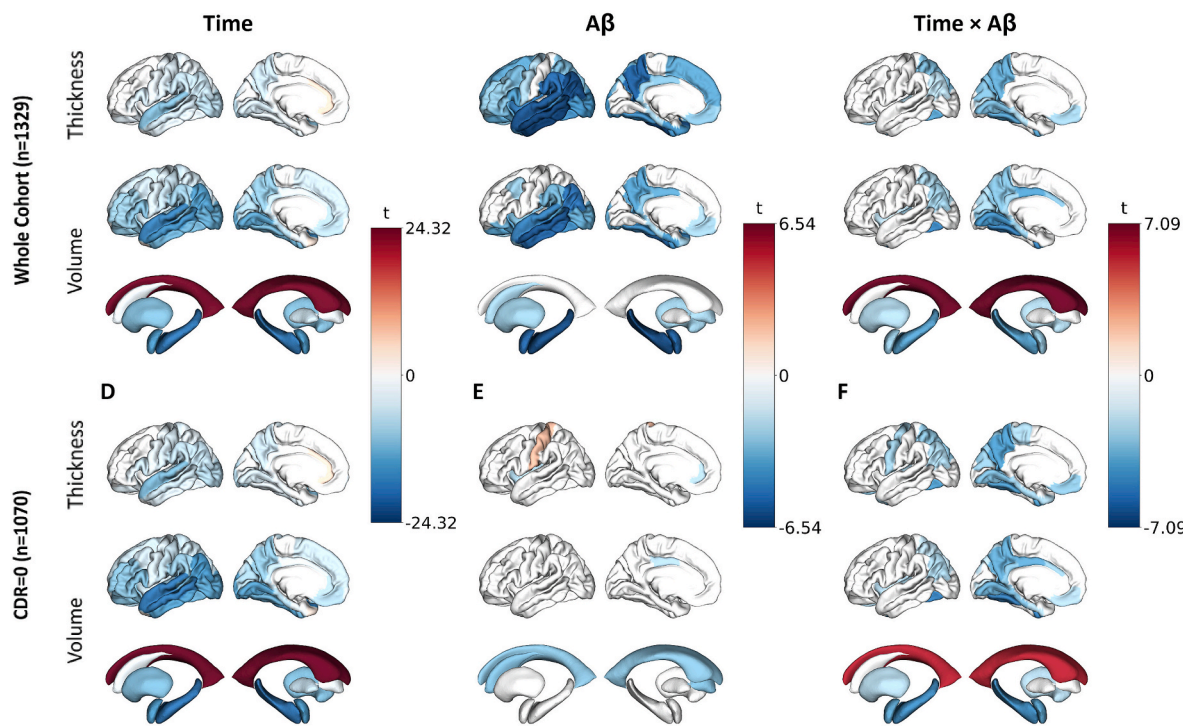


Fig. 1. Main & interaction effects of time & amyloid at baseline on regional volumes & thicknesses, in all participants and cognitively unimpaired (CDR = 0). Cortical mid-surface projections of FDR-thresholded LME main effects on cortical thickness, cortical volume and subcortical volume, of time (A) in all participants and (D) cognitively unimpaired (CDR = 0), main effect of baseline cortical A β (B) in all participants and (E) cognitively unimpaired (CDR = 0), and interaction effect of time and A β (C) in all participants and (F) cognitively unimpaired (CDR = 0). Surface projections show the lateral and medial cortex respectively, representative of averaged bilateral effects. A β , amyloid β ; CDR, Clinical Dementia Rating.

regression coefficients. The significance level was set at $\alpha < 0.05$ after applying the Benjamini-Hochberg procedure to correct for a false discovery rate within imaging phenotype, i.e. separately for thickness and volume. (Benjamini and Hochberg, 1995).

3. Results

Baseline demographics can be found in Table 1. The majority of individuals were cognitively unimpaired (CDR = 0; $N = 1070$, 81 %), with an overall average MMSE score of 28.82 (± 1.54). Mean age was 68.18 (± 8.78) years, 741 (56 %) were female, and 117/260 (8.8 %/19.6 %) were considered to have intermediate and elevated A β , respectively. Carriership of at least one allele of APOE- ϵ 4 was 40 % overall, with stepwise increases in carriership in the amyloid groups with 300/58/159 (32 %/51 %/66 %) APOE- ϵ 4 carriers in low, elevated and elevated A β participants, respectively. Follow-up time did not differ across amyloid groups with an overall median follow-up time of 3.4 (MD = 1.40) years, although overall availability of follow-up data differed between amyloid groups with more longitudinal data available for subjects with low A β (Supplementary Fig. 2). Individuals with elevated A β more frequently had a CDR = 0.5, lower MMSE scores, and a higher frequency of APOE- ϵ 4 carriership compared to low A β individuals. Only two individuals converted to CDR = 1 at follow-up, both of which had elevated A β at baseline. Sex- and APOE-stratified demographic characterizations can be found in Supplementary Table 1 and Supplementary Table 2, respectively. Male participants were older (68.81 years compared to 67.68 years), had higher educational level, and a larger proportion of very mild cognitive impairment (24 % compared to 16 %), but without any difference in MMSE or A β burden. People with one or more APOE- ϵ 4 allele were younger (66.56 years compared to 69.02 years), had higher proportion of very mild cognitive impairment (23 % compared to 16 %), lower MMSE (28.67 compared to 28.99), and higher A β burden (29.57CL compared to 11.33CL). Regional baseline SUVR and yearly

rates of change in A β groups as well as contrasted between sex and APOE- ϵ 4 are illustratively visualized in Supplementary Fig. 3, whereas regionalized atrophy rates (z/year) for these same subgroups are illustrated in Supplementary Fig. 4.

3.1. Effects of baseline A β burden on regional atrophy

LME results of the main models can be found in Supplementary Table 3 and are visualized in Fig. 1. Besides one significant positive effect of time on temporal pole volume, there was a significant negative main effect of time on all investigated cortical and subcortical gray matter volumes, suggesting widespread atrophy due to ageing-related neurodegeneration. This effect was most apparent in temporal and parietal regions as well as hippocampus and amygdala. Similar results were observed for cortical thickness, although posterior and anterior cingulate cortices showed thickening over time (Fig. 1A). All effects remained significant with comparable effect sizes in the CDR = 0 subset (Fig. 1D).

Higher baseline cortical amyloid burden was associated with lower baseline volumes at baseline in widespread AD signature regions, comprising lateral-temporal lobes, precuneus, posterior cingulate, amygdala, and hippocampus. These main effects and patterns also emerged for cortical thickness but were more distributed and stronger compared to volumes (Fig. 1B). These effects were largely absent in the CDR = 0 subset (Fig. 1E).

Longitudinally (Centiloid*Time), higher baseline cortical amyloid burden was related to a widespread decrease of volume and thickness at follow-up across regions, with the strongest interaction effects observed in the posterior cingulate, fusiform and parahippocampal gyri (Fig. 1C). Subcortically, this effect was most pronounced in the hippocampus and amygdala, followed by the putamen. Lateral ventricles showed progressive widening in relation to cortical amyloid burden. Except for hippocampal volume changes, most interaction effects were A β stage-

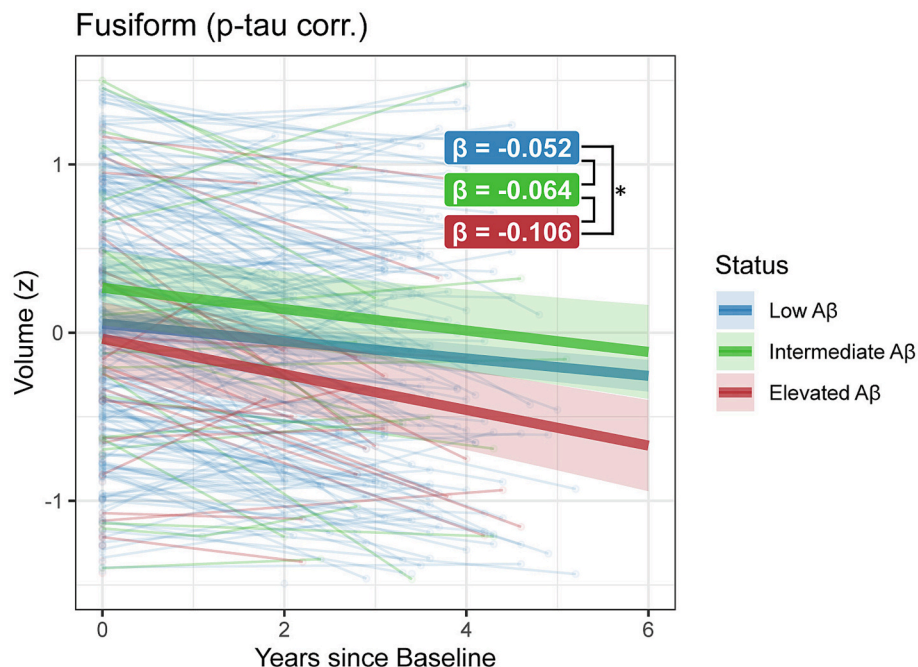


Fig. 2. Spaghetti plot of LME model effects of follow-up time on fusiform gyrus volume, stratified by amyloid status. Fusiform volume (z-scaled, residuals after correcting for age, sex, intracranial volume, CDR and p-tau181) is plotted against time (in years) since baseline amyloid-PET and MRI, stratified in low (<20CL), intermediate (20–40CL) and elevated Aβ (>40CL) groups. Fusiform atrophy is larger in participants with elevated Aβ compared to participants with low Aβ, independent of p-tau181. Aβ, amyloid β; CDR, Clinical Dementia Rating; PET, Positron Emission Tomography.

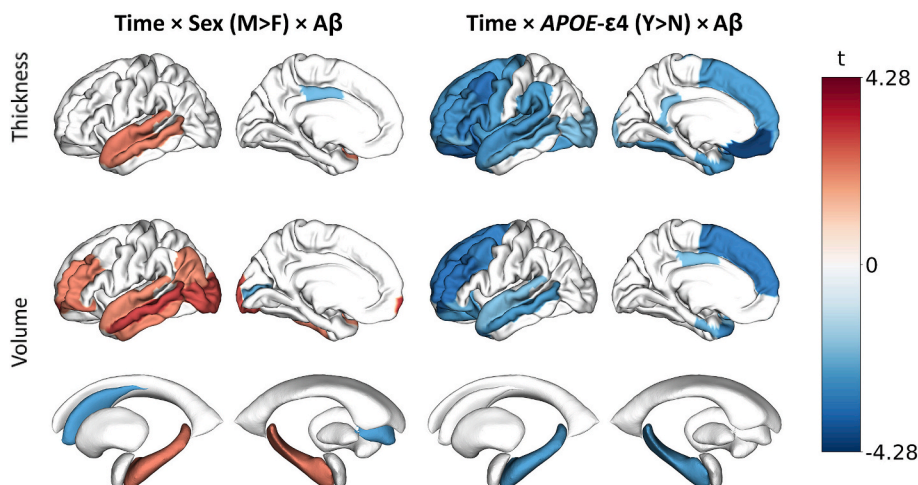


Fig. 3. Three-way interaction effects of time, Aβ burden at baseline and Sex or APOE-ε4 carriership on regional volumes & thicknesses. Cortical mid-surface projections of FDR-thresholded LME interaction effect t-values for cortical thickness, cortical volume and subcortical volume, of (A) time* $A\beta$ *sex, showing increased lateral and medial temporal atrophy for female compare to male participants with increases in Aβ, and (B) time* $A\beta$ *APOE-ε4, showing exacerbated atrophy for APOE-ε4 carriers in frontal and temporal regions. Surface projections show the lateral and medial cortex respectively, representative of averaged bilateral effects. Aβ, amyloid β.

dependent, with low and elevated Aβ groups showing significantly different slopes, but not low and intermediate Aβ groups. (Supplementary Fig. 5). In the CDR = 0 subset, most effects remained significant with slightly lower effect sizes (Fig. 1F).

In the CSF availability subset (N = 428), fewer Centiloid*Time interactions remained significant after FDR-correction, albeit with the same patterns (Supplementary Table 4). When correcting for t-tau or p-tau181, only fusiform volume atrophy remained significant (t-tau: $\beta = -0.011$, SE = 0.003, pFDR = 0.017; (p-tau: $\beta = -0.011$, SE = 0.003, pFDR = 0.017). Stratifying for amyloid status rather than continuous Centiloids, faster fusiform atrophy rates were found in participants with elevated compared to low Aβ burden ($\beta = -0.054$, SE = 0.017, pFDR = 0.006), but

not for participants with intermediate- compared to low Aβ ($\beta = -0.012$, SE = 0.019, pFDR = 0.801; Fig. 2).

3.2. Stratification by sex & APOE-ε4 carriership

To investigate the effect of sex and APOE-ε4 carriership, the LME models were expanded with three-way interactions (i.e., amyloid*time*sex and amyloid*time*APOE). Interaction effects between APOE-ε4 and time, sex and time, and APOE-ε4, sex and time are visualized in supplementary Fig. 4B and 4C. Over time, men had stronger loss of thickness in the superior temporal, inferior and superior parietal, and cuneus, as well as increased loss of volume in the caudate nucleus and

faster increase of lateral ventricle size. Women only had stronger atrophy in the caudal anterior cingulate gyrus. *APOE-ε4* carriers had decreased growth of lateral ventricle volume, and lower atrophy rates of entorhinal, temporal pole and frontal pole volume, as well as lower loss of frontal pole thickness. Effects of sex on the relationship between amyloid and brain atrophy were widespread (Fig. 3A). Women showed a generally exacerbated effect of $\text{A}\beta$ on atrophy compared to men, especially in lateral temporal regions and hippocampal volume ($\beta = 0.006$), with relatively less $\text{A}\beta$ -related atrophy only in the caudate nucleus ($\beta = -0.007$), pericalcarine volume ($\beta = -0.004$) and posterior cingulate thickness ($\beta = -0.008$). For *APOE-ε4*-carriers, more severe cortical thinning and loss of volume as a result of amyloid increase was observed compared to non-carriers (Fig. 3B) especially in frontal and lateral temporal regions as well as the hippocampus ($\beta = -0.007$).

3.3. Follow-Up $\text{A}\beta$ -PET data does not improve brain atrophy predictions

LME results of the data subset ($N = 684$) with available longitudinal $\text{A}\beta$ -PET are shown in [Supplementary Fig. 6A](#). Including follow-up PET scans generally did not improve predictions of volumetric or thickness measures, with significant improvements only in the prediction of volume of the posterior cingulate ($\Delta\text{AIC} = -9.55$), caudal-anterior cingulate ($\Delta\text{AIC} = -4.97$) and superior-frontal cortices ($\Delta\text{AIC} = -2.75$; [Supplementary Fig. 6B](#)).

4. Discussion

In this longitudinal prospective pan-European cohort study, we investigated the effect of baseline cortical $\text{A}\beta$ burden on subsequent cortical and subcortical brain atrophy in a large cohort of older adults with mostly preserved cognition. We showed that baseline $\text{A}\beta$ was predictive of widespread atrophy in several regions, most notably the medial-temporal lobes, fusiform, cingulate, and precuneus cortices. When correcting for p-tau or t-tau in a subset with available CSF data, only fusiform volume reductions were predicted by $\text{A}\beta$. Further, we demonstrated that amyloid-induced atrophy is exacerbated in women and with *APOE-ε4* carriership.

The observed widespread atrophy suggests an early effect of $\text{A}\beta$ on brain volume and thickness, and corroborates the importance of early intervention to prevent subsequent atrophy (Aisen et al., 2020). Amyloid-related longitudinal changes were observed at a comparable scale between volume and thickness, with the latter most prominently observed in the fusiform, precuneus, and superior temporal cortices, matching those ROI's previously selected in a cortical thickness *meta*-ROI to distinguish MCI/AD from healthy controls (Schwarz et al., 2016). In contrast, previous whole-brain investigations of the relationship between $\text{A}\beta$ and atrophy in preclinical or prodromal AD cohorts have largely focused on volume (Chételat et al., 2012; Tosun et al., 2011). These studies revealed similar affected regions, such as the precuneus, medial and lateral-temporal cortices, and posterior and middle cingulate. Clinical anti-amyloid trials mostly use global, lateral ventricle or hippocampal volumes as secondary outcomes (Rafii et al., 2023), and our results support the use of lateral ventricular and hippocampal volume to be potential surrogate outcomes in secondary prevention trials for subjects with elevated, but not intermediate levels of $\text{A}\beta$ burden. Importantly, baseline $\text{A}\beta$ remained predictive of fusiform atrophy after correcting for CSF p-tau181 or t-tau concentrations. Corroborating these results, a greater atrophy rate in the left fusiform independent of CSF p-tau181 was also previously found when comparing A-T- participants with normal cognition to A-T+ participants, with this effect absent in A-T+ individuals compared to either group (Cacciaglia et al., 2025). Taken together, these results are suggestive of a potential route of $\text{A}\beta$ -related atrophy independent of concurrent neurofibrillary tangles specifically in the fusiform gyrus, although other previous findings have found $\text{A}\beta$ -related fusiform atrophy to be exacerbated by tau presence without being completely independent of it (Nosheny et al., 2019). In

line, future fusiform tau deposition has previously been found to be predicted by $\text{A}\beta$ measured with Centiloid in both A-T- and A-T+ individuals (Cai et al., 2023), suggesting that increased $\text{A}\beta$ burden at baseline may lead to worse tau aggregation, which in turn would worsen atrophy, independently of baseline tau levels. The fusiform gyrus also being sensitive to general aging (Nosheny et al., 2019; Shah et al., 2021) and being among the first neocortical regions to atrophy in AD (Convit et al., 2000), the complex interplay between fusiform atrophy with aging, $\text{A}\beta$ and neurofibrillary tangles needs to be studied further. Conversely, the effect of $\text{A}\beta$ on regional atrophy was lost for all other regions when correcting for p-tau181 or t-tau, indicating that even in this early cohort, most of our observed atrophy is probably driven by the presence of fibrillary tau. A caveat of these sensitivity analyses is that p-tau181 is not only representative of neurofibrillary tangles, but also related to $\text{A}\beta$ burden itself (Salvadó et al., 2023), whilst t-tau is related to acute neuronal damage (Blennow and Zetterberg, 2018; Skillbäck et al., 2014); hence using these CSF markers as covariates may result in overcorrection. Novel CSF markers such as MTBR-tau243 have been found to be more specifically representative of neurofibrillary tangles and strongly linked to tau-PET burden (Horie et al., 2023). Future work should investigate the predictive value of $\text{A}\beta$ -PET for subsequent atrophy after correcting for MTBR-tau243.

When looking at the interacting effect of common candidate stratification factors in clinical trials, we found widespread sex-dependent effects with stronger amyloid-related atrophy in women, especially in medial and lateral temporal regions. Sauty and Durrellman (2023) previously found near-identical patterns of faster pace of atrophy in women in people with clinical diagnoses of AD, but not in MCI or cognitively unimpaired individuals, suggesting such an interaction effect to be predominant in late disease stages. Our present findings stem from a predominantly cognitively normal population, suggesting that clinical status may not drive accelerated atrophy in women as much as elevated pathological burden of at least $\text{A}\beta$, but likely also neurofibrillary tau: at comparable prevalence rates of tau-PET positivity between men and women (Ossenkoppele et al., 2025), women have been found to have larger quantities of neurofibrillary tangles in temporoparietal regions (Pereira et al., 2020) and faster rate of accumulation in inferior temporal and fusiform regions (Coughlan et al., 2025), suggesting that equal levels of $\text{A}\beta$ may lead to more neurofibrillary tau in women, leading subsequently to increased atrophy. We further observed that $\text{A}\beta$ -related atrophy is accelerated in *APOE-ε4* carriers, predominantly in frontal and temporal regions. Such *APOE-ε4*-related atrophy exacerbation has also been found in patients with AD, and in the superior temporal cortex also in people with MCI (Sauty and Durrellman, 2023). *APOE-ε4* predominance has also previously been reported in an AD frontal subtype of $\text{A}\beta$ accumulation (L. E. Collij et al., 2022); which, in light of our findings, could be suggestive of a spatial association between $\text{A}\beta$ deposition and downstream atrophy. In addition, given the increasingly established role of *APOE-ε4* in cerebrovascular (dys-)function (Tai et al., 2016) as well as a predominantly frontal pattern of vascular-related atrophy evident both independently of $\text{A}\beta$ and in $\text{A}\beta$ -positive participants (Heinen et al., 2020), underlying cerebrovascular pathology could well explain exacerbation of $\text{A}\beta$ -related atrophy in *APOE-ε4* carriers. How *APOE-ε4* impacts the potentially synergistic effect of amyloid- and cerebrovascular pathology needs to be studied further. Similarly, the subtle positive effects of *APOE-ε4* status after correction for $\text{A}\beta$ levels on entorhinal, temporal pole and frontal pole volumes as well as lateral ventricular volume we observed, although not intuitive, may reflect $\text{A}\beta$ -independent *APOE-ε4* mechanisms such as microglial activation (Ferrari-Souza et al., 2023), blood-brain barrier disruption (Montagne et al., 2020), or altered energy metabolism (Jackson et al., 2024), potentially leading to subtle cortical swelling due to neuroinflammation rather than true volume increases. Importantly, as phenotypes of macrostructural cortical changes, cortical volume is defined by both thickness and surface area, each with their own genetic underpinnings and cellular mechanisms (Panizzon et al., 2009). $\text{A}\beta$ -related volumetric change was

more diffusely exacerbated than thickness in women compared to men, warranting future research into changes of surface area, while A β -related cortical thinning was more exacerbated than volumetric loss in APOE- ϵ 4 carriers, suggesting these two phenotypes to be differently sensitive to AD risk factors and potentially reflecting slightly different neurodegenerative processes.

The observed cingulate thickening over time in our largely cognitively unimpaired, highly educated cohort may reflect a higher density of Von Economo neurons, which are especially concentrated in the cingulate gyrus and associated with well-maintained cognitive functioning (Allman et al., 2011; Gefen et al., 2018). This interpretation aligns with previous findings showing that greater cingulate thickness relates to a younger cognitive age and better cognitive performance (Pezzoli et al., 2024).

In the context of clinical trials, while a reduction of region-specific atrophy, namely hippocampal and lateral ventricular volume loss and fusiform thickness, could theoretically be the most detectable in patients with elevated A β levels over 40CL, existing successful anti-amyloid trials have reported either insignificant or accelerated volume decreases (Alves et al., 2023). These unexpected findings might be caused by off-target reduction of inflammatory responses, resulting in “pseudo-atrophy” (Barkhof and Knopman, 2023), with later discussions observing that such findings majorly occur in otherwise successful trials, designating it more specifically as “amyloid-removal related pseudo-atrophy” (Belder et al., 2024). While our findings highlight the importance of early anti-amyloid treatment to prevent detectable atrophy, atrophy itself would therefore likely not be a good outcome measure in anti-amyloid trials.

4.1. Limitations and future directions

Our findings represent the largest population to date to address the relationship between A β and atrophy in preclinical AD, enabling the inclusion of relevant covariates and stratification analyses such as the concurrent investigation of regional cortical volume and thickness. However, several methodological limitations need to be considered. First, the lack of a direct marker for neurofibrillary tangles, more closely related to patterns of atrophy in clinical AD than cortical A β (Gordon et al., 2018), did not allow us to disentangle the individual contributions of these pathological factors to brain atrophy. However, the observed associations in the CSF p-tau181 and t-tau sensitivity analyses as well as CDR = 0 subset analyses with a presumably relatively lower tau burden advocate for a partially independent effect of A β on neurodegeneration. The previously observed additive effect of vascular risk to the association between A β and atrophy was also not taken into account in this work and warrants future research (Rabin et al., 2022). Thirdly, we did not perform manual segmentation corrections of our FreeSurfer-derived cortical segmentations. While generally not altering region averages of the imaging phenotypes we investigated (McCarthy et al., 2015; Vahermaa et al., 2023), slight boundary errors have previously been found to be more prevalent in male participants, thus potentially introducing biases in our results (Vahermaa et al., 2023). Finally, the availability of follow-up data was skewed towards low A β burden participants, with over 80% of follow-up data coming from the low A β group at baseline (Supplementary Fig. 2). This bias may explain the overall lack of model improvement when including longitudinal PET data, as previous studies have highlighted the benefits of using follow-up PET data (Jagust et al., 2021). While the acquired data originated from 17 European sites and was acquired with different MRI scanners and A β -PET radiotracers, possible batch effects were minimized by utilizing state-of-the-art harmonization techniques (Fortin et al., 2018; Klunk et al., 2015).

In the present study, we investigated regional differences through the gyral based Desikan-Killiany atlas; future research could focus on more fine-grained parcellations such as hippocampal subfields, with more focal CA1, presubiculum and subiculum atrophy having been

shown to occur before other subfields in the amyloid cascade (Göschel et al., 2023; Zilioli et al., 2025). Additionally, as the global Centiloid metric is a robust measure (Shekari et al., 2024), commonly used in previous and ongoing trials and fully captures all early accumulating regions, we did not investigate regional measures of A β burden. However, evidence exists regarding the presence of different amyloid-PET spatial-temporal subtypes (L. E. Collij et al., 2022). It would be of interest to investigate whether regional amyloid-PET quantifications further improve atrophy prediction models, especially across more advanced disease stages. Beyond these aspects, rather than assuming a single pattern of atrophy due to A β , subtypes of atrophy (Risacher et al., 2017) in relation to A β accumulation alongside atrophy-related changes in cognitive functioning could be investigated.

4.2. Conclusions

We demonstrated the influence of cortical A β on brain atrophy in several regions in a population of older adults without dementia. Importantly, this influence was already exerted in cognitively unimpaired individuals and was exacerbated in women and APOE ϵ 4 carriers. Our results highlight cortical thickness and volume as differentially affected biomarkers of macroscale atrophy. Overall, our findings emphasize the importance of early intervention strategies to mitigate A β -related neurodegeneration, with implications for the design and interpretation of clinical trials aimed at preventing AD.

CRediT authorship contribution statement

Leonard Pieperhoff: Writing – review & editing, Writing – original draft, Visualization, Methodology, Investigation, Formal analysis, Conceptualization. **Luigi Lorenzini:** Writing – review & editing, Visualization, Supervision, Methodology, Conceptualization. **Sophie Mastenbroek:** Writing – review & editing, Methodology, Formal analysis, Conceptualization. **Mario Tranza:** Writing – review & editing, Methodology. **Mahnaz Shekari:** Writing – review & editing, Methodology, Data curation. **Alle Meije Wink:** Writing – review & editing, Supervision, Methodology, Data curation. **Robin Wolz:** Writing – review & editing, Software, Resources, Funding acquisition. **Sylke Grootoorn:** Writing – review & editing, Software, Resources. **Craig Ritchie:** Writing – review & editing, Funding acquisition. **Mercè Boada:** Writing – review & editing, Funding acquisition. **Marta Marquié:** Writing – review & editing, Funding acquisition. **Wiesje van der Flier:** Writing – review & editing, Funding acquisition. **Rik Vandenberghe:** Writing – review & editing, Funding acquisition. **Bernard J. Hanseeuw:** Writing – review & editing, Funding acquisition. **Pablo Martínez-Lage:** Writing – review & editing, Funding acquisition. **Pierre Payoux:** Writing – review & editing, Funding acquisition. **Pieter Jelle Visser:** Writing – review & editing, Funding acquisition. **Michael Schöll:** Writing – review & editing, Funding acquisition. **Giovanni B. Frisoni:** Writing – review & editing, Funding acquisition. **Andrew Stephens:** Writing – review & editing, Resources, Funding acquisition. **Christopher Buckley:** Writing – review & editing, Resources, Funding acquisition. **Gill Farrar:** Writing – review & editing, Resources, Funding acquisition. **Frank Jessen:** Writing – review & editing, Funding acquisition. **Oriol Grau-Rivera:** Writing – review & editing, Methodology. **Juan Domingo Gispert:** Writing – review & editing, Funding acquisition. **David Vállez García:** Writing – review & editing, Project administration, Methodology, Data curation. **Henk Mutsaerts:** Writing – review & editing, Supervision. **Frederik Barkhof:** Writing – review & editing, Supervision, Funding acquisition. **Lyduine E. Collij:** Writing – review & editing, Supervision, Methodology, Funding acquisition.

Appendix A. Supplementary data

Supplementary data to this article can be found online at <https://doi.org/10.1016/j.nicl.2025.103912>.

Data availability

Data for this study were drawn from the AMYPAD PNHS v202306, available on the AD Workbench and can be requested via the AD Workbench FAIR portal under https://fair.addi.addatainitiative.org/#/data/datasets/amypad_pnhs_harmonised_and_derived_v202306. The data access request procedure is described under <https://doi.org/10.5281/zenodo.7962924>.

References

- Aisen, P.S., Cummings, J., Doody, R., Kramer, L., Salloway, S., Selkoe, D.J., Sims, J., Sperling, R.A., Vellas, B., 2020. The Future of Anti-Amyloid Trials. *J. Prev Alzheimers Dis.* 7, 146–151. <https://doi.org/10.14283/jpad.2020.24>.
- Allman, J.M., Tetreault, N.A., Hakeem, A.Y., Park, S., 2011. The von Economo neurons in apes and humans. *Am. J. Hum. Biol.* 23, 5–21. <https://doi.org/10.1002/ajhb.21136>.
- Alves, F., Kalinowski, P., Ayton, S., 2023. Accelerated Brain volume loss Caused by Anti- β -Amyloid drugs: a Systematic Review and Meta-analysis. *Neurology* 100, e2114–e2124. <https://doi.org/10.1212/WNL.000000000000207268>.
- Barkhof, F., Knopman, D.S., 2023. Brain Shrinkage in Anti- β -Amyloid Alzheimer Trials: Neurodegeneration or Pseudoatrophy?: *Neurology*: Vol 100, No 20. *Neurology* 100, 941–942. <https://doi.org/10.1212/WNL.000000000000207268>.
- Barthel, H., Gertz, H.-J., Dresel, S., Peters, O., Bartenstein, P., Buerger, K., Hiemeyer, F., Wittemer-Rump, S.M., Seibyl, J., Reiningher, C., Sabri, O., Florbetaben Study Group, 2011. Cerebral amyloid- β PET with florbetaben (18F) in patients with Alzheimer's disease and healthy controls: a multicentre phase 2 diagnostic study. *Lancet Neurol.* 10, 424–435. [https://doi.org/10.1016/S1474-4422\(11\)70077-1](https://doi.org/10.1016/S1474-4422(11)70077-1).
- Bejanin, A., Schonhaut, D.R., La Joie, R., Kramer, J.H., Baker, S.L., Sosa, N., Ayakta, N., Cantwell, A., Janabi, M., Lauriola, M., O'Neil, J.P., Gorno-Tempini, M.L., Miller, Z. A., Rosen, H.J., Miller, B.L., Jagust, W.J., Rabinovici, G.D., 2017. Tau pathology and neurodegeneration contribute to cognitive impairment in Alzheimer's disease. *Brain* 140, 3286–3300. <https://doi.org/10.1093/brain/awx243>.
- Belder, C.R.S., Boche, D., Nicoll, J.A.R., Jaunmuktane, Z., Zetterberg, H., Schott, J.M., Barkhof, F., Fox, N.C., 2024. Brain volume change following anti-amyloid β immunotherapy for Alzheimer's disease: amyloid-removal-related pseudo-atrophy. *Lancet Neurol.* 23, 1025–1034. [https://doi.org/10.1016/S1474-4422\(24\)00335-1](https://doi.org/10.1016/S1474-4422(24)00335-1).
- Benjamini, Y., Hochberg, Y., 1995. Controlling the false discovery rate: a practical and powerful approach to multiple testing. *J. R. Stat. Soc. Ser. B Stat. Methodol.* 57, 289–300. <https://doi.org/10.1111/j.2517-6161.1995.tb02031.x>.
- Blennow, K., Zetterberg, H., 2018. Biomarkers for Alzheimer's disease: current status and prospects for the future. *J. Intern. Med.* 284, 643–663. <https://doi.org/10.1111/joim.12816>.
- Bocaneca, D.I., den Braber, A., Jiang, C., Coomans, E.M., van Unnik, A.A.J.M., van Veen, J.M.L., Ribberink, M., Reijner, N., Saddal, S., Mastenbroek, S.E., van Gils, A. M., Kluin, C.M., de Leeuw, D.M., Vromen, E.M., Bekkers, L., Georgallidou, M., van der Landen, S.M., Baumann, J.M., Heuvelink, J., Reus, L.M., Lorenzini, L., Kamps, S., Bouman, S.P.H., Singleton, E.H., de Boer, S.C.M., Rousset, R.Z., Kuijper, B., Verhagen, E., Smit, D., Rikken, R.M., Visser, P.J., Bouwman, F.H., Barkhof, F., Lemstra, A.W., Pijnenburg, Y.A.L., van der Flier, W.M., Venkatraghavan, V., Tijms, B.M., 2023. Automated FreeSurfer segmentation and visual quality control in 10,000 MRI scans from a large memory clinic cohort. *Alzheimers Dement.* 19, <https://doi.org/10.1002/ald.078805>.
- Buckley, R.F., Mormino, E.C., Rabin, J.S., Hohman, T.J., Landau, S., Hanseeuw, B.J., Jacobs, H.I.L., Papp, K.V., Amariglio, R.E., Properzi, M.J., Schultz, A.P., Kirn, D., Scott, M.R., Hedden, T., Farrell, M., Price, J., Chhatwal, J., Rentz, D.M., Villemagne, V.L., Johnson, K.A., Sperling, R.A., 2019. Sex differences in the Association of Global Amyloid and Regional Tau Deposition Measured by Positron Emission Tomography in Clinically Normal older adults. *JAMA Neurol.* 76, 542–551. <https://doi.org/10.1001/jamaneurol.2018.4693>.
- Cacciaglia, R., Falcón, C., Benavides, G.S., Brugulat-Serrat, A., Alomà, M.M., Calvet, M. S., Molinuevo, J.L., Fauria, K., Minguillón, C., Kollmorgen, G., Quijano-Rubio, C., Blennow, K., Zetterberg, H., Lorenzini, L., Wink, A.M., Ingala, S., Barkhof, F., Ritchie, C.W., Gispert, J.D., 2025. ALFA study, Soluble A β pathology predicts neurodegeneration and cognitive decline independently on p-tau in the earliest Alzheimer's continuum: evidence across two independent cohorts. *Alzheimers Dement.* 21, e14415. <https://doi.org/10.1002/alz.14415>.
- Cai, Y., Du, J., Li, A., Zhu, Y., Xu, L., Sun, K., Ma, S., Guo, T., 2023. Alzheimer's Disease Neuroimaging Initiative, Initial levels of β -amyloid and tau deposition have distinct effects on longitudinal tau accumulation in Alzheimer's disease. *Alzheimers Res. Ther.* 15, 30. <https://doi.org/10.1186/s13195-023-01178-w>.
- Chételat, G., Villemagne, V.L., Pike, K.E., Baron, J.-C., Bourgeat, P., Jones, G., Faux, N.G., Ellis, K.A., Salvado, O., Szoekie, C., Martins, R.N., Ames, D., Masters, C.L., Rowe, C. C., Australian Imaging Biomarkers and Lifestyle Study of Ageing (AIBL) Research Group, 2010. Larger temporal volume in elderly with high versus low beta-amyloid deposition. *Brain* 133, 3349–3358. <https://doi.org/10.1093/brain/awp187>.
- Chételat, G., Villemagne, V.L., Villain, N., Jones, G., Ellis, K.A., Ames, D., Martins, R.N., Masters, C.L., Rowe, C.C., AIBL Research Group, 2012. Accelerated cortical atrophy in cognitively normal elderly with high β -amyloid deposition. *Neurology* 78, 477–484. <https://doi.org/10.1212/WNL.0b013e318246d67a>.
- Collij, L.E., Farrar, G., Valléz García, D., Bader, I., Shekari, M., Lorenzini, L., Pemberton, H., Altomare, D., Pla, S., Loor, M., Markiewicz, P., Yaqub, M., Buckley, C., Frisoni, G.B., Nordberg, A., Payoux, P., Stephens, A., Gismondi, R., Visser, P.J., Ford, L., Schmidt, M., Birck, C., Georges, J., Mett, A., Walker, Z., Boada, M., Drzezga, A., Vandenberghe, R., Hanseeuw, B., Jessen, F., Schöll, M., Ritchie, C., Lopes Alves, I., Gispert, J.D., Barkhof, F., 2022a. The amyloid imaging for the prevention of Alzheimer's disease consortium: a European collaboration with global impact. *Front. Neurol.* 13, 1063598. <https://doi.org/10.3389/fneur.2022.1063598>.
- Collij, L.E., Salvadó, G., Shekari, M., Lopes Alves, I., Reimand, J., Wink, A.M., Zwan, M., Niñerola-Baizán, A., Perissinotti, A., Scheltens, P., Ikonomicov, M.D., Smith, A.P.L., Farrar, G., Molinuevo, J.L., Barkhof, F., Buckley, C.J., van Berckel, B.N.M., Gispert, J.D., 2021. ALFA study, AMYPAD consortium, Visual assessment of [18F] flutemetamol PET images can detect early amyloid pathology and grade its extent. *Eur. J. Nucl. Med. Mol. Imaging* 48, 2169–2182. <https://doi.org/10.1007/s00259-020-05174-2>.
- Collij, L.E., Salvadó, G., Wottschel, V., Mastenbroek, S.E., Schoenmakers, P., Heeman, F., Aksman, L., Wink, A.M., Berckel, B.N.M., Flier, W.M., Scheltens, P., Visser, P.J., Barkhof, F., Haller, S., Gispert, J.D., Lopes Alves, I., 2022b. Spatial-Temporal patterns of β -Amyloid Accumulation: a Subtype and Stage Inference Model Analysis. *Neurology* 98. <https://www.neurology.org/doi/10.1212/WNL.000000000000200148>.
- Convit, A., de Asis, J., de Leon, M.J., Tarshish, C.Y., De Santi, S., Rusinek, H., 2000. Atrophy of the medial occipitotemporal, inferior, and middle temporal gyri in non-demented elderly predict decline to Alzheimer's disease. *Neurobiol. Aging* 21, 19–26. [https://doi.org/10.1016/S0197-4580\(99\)00107-4](https://doi.org/10.1016/S0197-4580(99)00107-4).
- Coughlan, G.T., Klinger, H.M., Boyle, R., Betthauser, T.J., Binette, A.P., Christenson, L., Chadwick, T., Hansson, O., Harrison, T.M., Healy, B., Jacobs, H.I.L., Hanseeuw, B., Jonaitis, E., Jack Jr, C.R., Johnson, K.A., Langhough, R.E., Properzi, M.J., Rentz, D. M., Schultz, A.P., Smith, R., Seto, M., Johnson, S.C., Mielke, M.M., Shirzadi, Z., Yau, W.-Y.-W., Manson, J.E., Sperling, R.A., Vemuri, P., Buckley, R.F., 2025. Alzheimer's Disease Neuroimaging Initiative, Sex differences in longitudinal tau-PET in preclinical Alzheimer disease: a meta-analysis. *JAMA Neurol.* 82, 364. <https://doi.org/10.1001/jamaneurol.2025.0013>.
- Curtis, C., Gamez, J.E., Singh, U., Sadowsky, C.H., Villena, T., Sabbagh, M.N., Beach, T. G., Duara, R., Fleisher, A.S., Frey, K.A., Walker, Z., Hunjan, A., Holmes, C., Escovar, Y.M., Vera, C.X., Agronin, M.E., Ross, J., Bozoki, A., Aklinola, M., Shi, J., Vandenberghe, R., Ikonomicov, M.D., Sherwin, P.F., Grachev, I.D., Farrar, G., Smith, A.P.L., Buckley, C.J., McLain, R., Salloway, S., 2015. Phase 3 trial of flutemetamol labeled with radioactive fluorine 18 imaging and neuritic plaque density. *JAMA Neurol.* 72, 287–294. <https://doi.org/10.1001/jamaneurol.2014.4144>.
- Desikan, R.S., Ségonne, F., Fischl, B., Quinn, B.T., Dickerson, B.C., Blacker, D., Buckner, R.L., Dale, A.M., Maguire, R.P., Hyman, B.T., Albert, M.S., Killiany, R.J., 2006. An automated labeling system for subdividing the human cerebral cortex on MRI scans into gyral based regions of interest. *Neuroimage* 31, 968–980. <https://doi.org/10.1016/j.neuroimage.2006.01.021>.
- Dhamala, E., Ooi, L.Q.R., Chen, J., Kong, R., Anderson, K.M., Chin, R., Yeo, B.T.T., Holmes, A.J., 2022. Proportional intracranial volume correction differentially biases behavioral predictions across neuroanatomical features, sexes, and development. *Neuroimage* 260, 119485. <https://doi.org/10.1016/j.neuroimage.2022.119485>.
- Ferrari-Souza, J.P., Lussier, F.Z., Leffa, D.T., Therriault, J., Tissot, C., Bellaver, B., Ferreira, P.C.L., Malpetti, M., Wang, Y.-T., Povala, G., Benedet, A.L., Ashton, N.J., Chamoun, M., Servesa, S., Bezgin, G., Kang, M.S., Stevenson, J., Rahmouni, N., Pallen, V., Poltronetti, N.M., O'Brien, J.T., Rowe, J.B., Cohen, A.D., Lopez, O.L., Tudorascu, D.L., Karikari, T.K., Klunk, W.E., Villemagne, V.L., Soucy, J.-P., Gauthier, S., Souza, D.O., Zetterberg, H., Blennow, K., Zimmer, E.R., Rosa-Neto, P., Pascoa, T.A., 2023. APOE ϵ 4 associates with microglial activation independently of A β plaques and tau tangles. *Sci. Adv.* 9, eade1474. <https://doi.org/10.1126/sciadv.ade1474>.
- Fortin, J.-P., Cullen, N., Sheline, Y.I., Taylor, W.D., Aselcioglu, I., Cook, P.A., Adams, P., Cooper, C., Fava, M., McGrath, P.J., McInnis, M., Phillips, M.L., Trivedi, M.H., Weissman, M.M., Shinohara, R.T., 2018. Harmonization of cortical thickness measurements across scanners and sites. *Neuroimage* 167, 104–120. <https://doi.org/10.1016/j.neuroimage.2017.11.024>.
- García, D.V., 2023. AMYPAD PNHS - Integrated dataset (Raw) v202306. <https://doi.org/10.5281/ZENODO.8017084>.
- Gefen, T., Papastefan, S.T., Rezvanian, A., Bigio, E.H., Weintraub, S., Rogalski, E., Mesulam, M.-M., Geula, C., 2018. Von Economo neurons of the anterior cingulate across the lifespan and in Alzheimer's disease. *Cortex* 99, 69–77. <https://doi.org/10.1016/j.cortex.2017.10.015>.
- Gordon, B.A., McCullough, A., Mishra, S., Blazey, T.M., Su, Y., Christensen, J., Dincer, A., Jackson, K., Hornbeck, R.C., Morris, J.C., Ances, B.M., Benzinger, T.L.S., 2018. Cross-sectional and longitudinal atrophy is preferentially associated with tau rather than amyloid β positron emission tomography pathology. *Alzheimers Dement.* 10, 245–252. <https://doi.org/10.1016/j.jad.2018.02.003>.
- Göschel, L., Kurz, L., Dell'Orco, A., Köbe, T., Körtvélyessy, P., Fillmer, A., Aydin, S., Riemann, L.T., Wang, H., Ittermann, B., Grittner, U., Flöel, A., 2023. 7T amygdala and hippocampus subfields in volumetry-based associations with memory: a 3-year follow-up study of early Alzheimer's disease. *NeuroImage Clin.* 38, 103439. <https://doi.org/10.1016/j.nic.2023.103439>.
- Gustavsson, A., Norton, N., Fast, T., Fröhlich, L., Georges, J., Holzapfel, D., Kirabali, T., Krolak-Salmon, P., Rossini, P.M., Ferretti, M.T., Lanman, L., Chadha, A.S., van der Flier, W.M., 2023. Global estimates on the number of persons across the Alzheimer's disease continuum. *Alzheimers Dement.* 19, 658–670. <https://doi.org/10.1002/alz.12694>.
- Heinen, R., Groeneweld, O.N., Barkhof, F., de Bresser, J., Exalto, L.G., Kuijff, H.J., Prins, N.D., Scheltens, P., van der Flier, W.M., Biessels, G.J., 2020. TRACE-VCI study group, Small vessel disease lesion type and brain atrophy: the role of co-occurring amyloid. *Alzheimers Dement. (amst.)* 12, e12060. <https://doi.org/10.1002/dad2.12060>.

- Horie, K., Salvadó, G., Barthélémy, N.R., Janelidze, S., Li, Y., He, Y., Saef, B., Chen, C.D., Jiang, H., Strandberg, O., Pichet Binette, A., Palmqvist, S., Sato, C., Sachdev, P., Koyama, A., Gordon, B.A., Benzinger, T.L.S., Holtzman, D.M., Morris, J.C., Mattsson-Carlsgren, N., Stomrud, E., Ossenkoppele, R., Schindler, S.E., Hansson, O., Bateman, R.J., 2023. CSF MTBR-tau243 is a specific biomarker of tau tangle pathology in Alzheimer's disease. *Nat. Med.* 29, 1954–1963. <https://doi.org/10.1038/s41591-023-02443-z>.
- Ingala, S., De Boer, C., Masselink, L.A., Vergari, I., Lorenzini, L., Blennow, K., Chételat, G., Di Perri, C., Ewers, M., van der Flier, W.M., Fox, N.C., Gispert, J.D., Haller, S., Molinuevo, J.L., Muniz-Terrera, G., Mutsaerts, H.J., Ritchie, C.W., Ritchie, K., Schmidt, M., Schwarz, A.J., Vermunt, L., Waldman, A.D., Wardlaw, J., Wink, A.M., Wolz, R., Wottschel, V., Scheltens, P., Visser, P.J., Barkhof, F., 2021. EPAD consortium, Application of the ATN classification scheme in a population without dementia: Findings from the EPAD cohort. *Alzheimers Dement.* 17, 1189–1204. <https://doi.org/10.1002/alz.12292>.
- Jack Jr, C.R., Wiste, H.J., Weigand, S.D., Therneau, T.M., Lowe, V.J., Knopman, D.S., Gunter, J.L., Senjem, M.L., Jones, D.T., Kantarci, K., Machulda, M.M., Mielke, M.M., Roberts, R.O., Vemuri, P., Reyes, D.A., Petersen, R.C., 2017. Defining imaging biomarker cut points for brain aging and Alzheimer's disease. *Alzheimers Dement.* 13, 205–216. <https://doi.org/10.1016/j.jalz.2016.08.005>.
- Jackson, R.J., Hyman, B.T., Serrano-Pozo, A., 2024. Multifaceted roles of APOE in Alzheimer disease. *Nat. Rev. Neurol.* 20, 457–474. <https://doi.org/10.1038/s41582-024-00988-2>.
- Jagust, W.J., Landau, S.M., 2021. Alzheimer's Disease Neuroimaging Initiative, Temporal Dynamics of β -Amyloid Accumulation in Aging and Alzheimer Disease. *Neurology* 96, e1347–e1357. <https://doi.org/10.1212/WNL.00000000000011524>.
- Josephs, K.A., Whitwell, J.L., Ahmed, Z., Shiung, M.M., Weigand, S.D., Knopman, D.S., Boeve, B.F., Parisi, J.E., Petersen, R.C., Dickson, D.W., Jack Jr, C.R., 2008. Beta-amyloid burden is not associated with rates of brain atrophy. *Ann. Neurol.* 63, 204–212. <https://doi.org/10.1002/ana.21223>.
- Kepp, K.P., Sensi, S.L., Johnsen, K.B., Barrio, J.R., Høilund-Carlsen, P.F., Neve, R.L., Alavi, A., Herrup, K., Perry, G., Robakis, N.K., Vissel, B., Espay, A.J., 2023. The Anti-Amyloid Monoclonal Antibody Lecanemab: 16 Cautionary Notes. *J. Alzheimers Dis.* 94, 497–507. <https://doi.org/10.3233/JAD-230099>.
- Klunk, W.E., Koeppe, R.A., Price, J.C., Benzinger, T.L., Devous Sr, M.D., Jagust, W.J., Johnson, K.A., Mathis, C.A., Minhas, D., Pontecorvo, M.J., Rowe, C.C., Skovronsky, D.M., Mintun, M.A., 2015. The Centiloid Project: standardizing quantitative amyloid plaque estimation by PET. *Alzheimers Dement.* 11 (1–15), e1–e4. <https://doi.org/10.1016/j.jalz.2014.07.003>.
- La Joie, R., Visani, A.V., Baker, S.L., Brown, J.A., Bourakova, V., Cha, J., Chaudhary, K., Edwards, L., Iaccarino, L., Janabi, M., Lesman-Segev, O.H., Miller, Z.A., Perry, D.C., O'Neil, J.P., Pham, J., Rojas, J.C., Rosen, H.J., Seeley, W.W., Tsai, R.M., Miller, B.L., Jagust, W.J., Rabinovici, G.D., 2020. Prospective longitudinal atrophy in Alzheimer's disease correlates with the intensity and topography of baseline tau-PET. *Sci. Transl. Med.* 12. <https://doi.org/10.1126/scitranslmed.aaa5732>.
- Lopes Alves, I., Collij, L.E., Altomare, D., Frisoni, G.B., Saint-Aubert, L., Payoux, P., Kivipelto, M., Jessen, F., Drzezga, A., Leeuwis, A., Wink, A.M., Visser, P.J., van Berckel, B.N.M., Scheltens, P., Gray, K.R., Wolz, R., Stephens, A., Gismondi, R., Buckley, C., Gispert, J.D., Schmidt, M., Ford, L., Ritchie, C., Farrar, G., Barkhof, F., Molinuevo, J.L., AMYPAD Consortium, 2020. Quantitative amyloid PET in Alzheimer's disease: the AMYPAD prognostic and natural history study. *Alzheimers Dement.* 16, 750–758. <https://doi.org/10.1002/alz.12069>.
- Martikainen, I.K., Kemppainen, N., Johansson, J., Teuho, J., Helin, S., Liu, Y., Helisalmi, S., Soininen, H., Parkkola, R., Ngandu, T., Kivipelto, M., Rinne, J.O., 2019. Brain β -Amyloid and Atrophy in individuals at increased risk of Cognitive Decline. *AJNR Am. J. Neuroradiol.* 40, 80–85. <https://doi.org/10.3174/ajnr.A5891>.
- Mattsson, N., Eriksson, O., Lindberg, O., Schöll, M., Lampinen, B., Nilsson, M., Insel, P.S., Lautner, R., Strandberg, O., van Westen, D., Zetterberg, H., Blennow, K., Palmqvist, S., Stomrud, E., Hansson, O., 2018. Effects of APOE e4 on neuroimaging, cerebrospinal fluid biomarkers, and cognition in prodromal Alzheimer's disease. *Neurobiol. Aging* 71, 81–90. <https://doi.org/10.1016/j.neurobiolaging.2018.07.003>.
- Mattsson, N., Insel, P.S., Nosheny, R., Tosun, D., Trojanowski, J.Q., Shaw, L.M., Jack Jr, C.R., Donohue, M.C., Weiner, M.W., 2014. Alzheimer's Disease Neuroimaging Initiative, Emerging β -amyloid pathology and accelerated cortical atrophy. *JAMA Neurol.* 71, 725–734. <https://doi.org/10.1001/jamaneurol.2014.446>.
- McCarthy, C.S., Ramprashad, A., Thompson, C., Botti, J.-A., Coman, I.L., Kates, W.R., 2015. A comparison of FreeSurfer-generated data with and without manual intervention. *Front. Neurosci.* 9, 379. <https://doi.org/10.3389/fnins.2015.00379>.
- Montagne, A., Nation, D.A., Sagare, A.P., Barisano, G., Sweeney, M.D., Chakhoyan, A., Pachicano, M., Joe, E., Nelson, A.R., D'Orazio, L.M., Buennagel, D.P., Harrington, M.G., Benzinger, T.L.S., Fagan, A.M., Ringman, J.M., Schneider, L.S., Morris, J.C., Reiman, E.M., Caselli, R.J., Chui, H.C., Tcw, J., Chen, Y., Pa, J., Conti, P.S., Law, M., Toga, A.W., Zlokovic, B.V., 2020. APOE4 leads to blood-brain barrier dysfunction predicting cognitive decline. *Nature* 581, 71–76. <https://doi.org/10.1038/s41586-020-2247-3>.
- Nosheny, R.L., Insel, P.S., Mattsson, N., Tosun, D., Buckley, S., Truran, D., Schuff, N., Aisen, P.S., Weiner, M.W., 2019. Alzheimer's Disease Neuroimaging Initiative, Associations among amyloid status, age, and longitudinal regional brain atrophy in cognitively unimpaired older adults. *Neurobiol. Aging* 82, 110–119. <https://doi.org/10.1016/j.neurobiolaging.2019.07.005>.
- Ossenkoppele, R., Coomans, E.M., Apostolova, L.G., Baker, S.L., Barthel, H., Beach, T.G., Benzinger, T.L.S., Bethausser, T., Bischoff, G.N., Bottlaender, M., Bourgeat, P., den Braber, A., Brendel, M., Brickman, A.M., Cash, D.M., Carrillo, M.C., Coath, W., Christian, B.T., Dickerson, B.C., Dore, V., Drzezga, A., Feizpour, A., van der Flier, W., M., Franzmeier, N., Frisoni, G.B., Garibotto, V., van de Giessen, E., Domingo-Gispert, J., Gnoerich, J., Gu, Y., Guan, Y., Hanseeuw, B.J., Harrison, T.M., Jack, C.R., Jaeger, E., Jagust, W.J., Jansen, W.J., La Joie, R., Johnson, K.A., Johnson, S.C., Kennedy, I., A., Kim, J.P., van Laere, K., Lagarde, J., Lao, P., Luchsinger, J.A., Kern, S., Kreisl, W., C., Malotaux, V., Malpetti, M., Manly, J.J., Mao, X., Mattsson-Carlsgren, N., Mayo Clinic Study on Aging, Messerschmidt, K., Minguillon, C., Mormino, E.M., O'Brien, J., T., Palmqvist, S., Petersen, D.E., Petersen, R.C., Pijnenburg, Y.A.L., Pontecorvo, M.J., Poirier, J., PREVENT-AD Research Group, Rabinovici, G.D., Rahmouni, N., Risacher, S.L., Rosa-Neto, P., Rosen, H., Rowe, C.C., Rowe, J.B., Rullmann, M., Salman, Y., Sarazin, M., Saykin, A.J., Schneider, J.A., Schöll, M., Schott, J.M., Seo, S.W., Serrano, G.E., Shcherbinin, S., Shekari, M., Skoog, I., Smith, R., Sperling, R.A., Spruyt, L., Stomrud, E., Strandberg, O., Therriault, J., Xie, F., Vandenberghe, R., Villemagne, V., L., Villeneuve, S., Visser, P.J., Vossler, H., Young, C.B., Groot, C., Hansson, O., 2025. Tau PET positivity in individuals with and without cognitive impairment varies with age, amyloid- β status, APOE genotype and sex. *Nat. Neurosci.* 28, 1610–1621. <https://doi.org/10.1038/s41593-025-02000-6>.
- Panizzon, M.S., Fennema-Notestine, C., Eyler, L.T., Jernigan, T.L., Prom-Wormley, E., Neale, M., Jacobson, K., Lyons, M.J., Grant, M.D., Franz, C.E., Xian, H., Tsuang, M., Fischl, B., Seidman, L., Dale, A., Kremen, W.S., 2009. Distinct genetic influences on cortical surface area and cortical thickness. *Cereb. Cortex* 19, 2728–2735. <https://doi.org/10.1093/cercor/bhp026>.
- Pereira, J.B., Harrison, T.M., La Joie, R., Baker, S.L., Jagust, W.J., 2020. Spatial patterns of tau deposition are associated with amyloid, ApoE, sex, and cognitive decline in older adults. *Eur. J. Nucl. Med. Mol. Imaging* 47, 2155–2164. <https://doi.org/10.1007/s00259-019-04669-x>.
- Pezzoli, S., Giorgio, J., Martersteck, A., Dobyns, L., Harrison, T.M., Jagust, W.J., 2024. Successful cognitive aging is associated with thicker anterior cingulate cortex and lower tau deposition compared to typical aging. *Alzheimers Dement.* 20, 341–355. <https://doi.org/10.1002/alz.13438>.
- P.R. Raamana A. Theyers T. Selliah P. Bhati S.R. Arnott S. Hassel N.D. Nanayakkara M. Scott C.J., Harris, J., Zamyadi, M., Lam, R.W., Milev, R., Müller, D.J., Rotzinger, S., Frey, B.N., Kennedy, S.H., Black, S.E., Lang, A., Masellis, M., Symons, S., Bartha, R., MacQueen, G.M., C. Strother, S., Visual QC protocol for FreeSurfer cortical parcellations from anatomical MRI Aperture Neuro. <https://doi.org/10.1101/10.52294/1cdce19c-e6db-4684-97cb-ae709da06a3f>.
- Rabin, J.S., Pruzin, J., Scott, M., Yang, H.-S., Hampton, O., Hsieh, S., Schultz, A.P., Buckley, R.F., Hedden, T., Rentz, D., Johnson, K.A., Sperling, R.A., Chhatwal, J.P., 2022. Association of β -amyloid and vascular risk on longitudinal patterns of brain atrophy. *Neurology* 99, e270–e280. <https://doi.org/10.1212/WNL.00000000000020051>.
- Raffi, M.S., Sperling, R.A., Donohue, M.C., Zhou, J., Roberts, C., Irizarry, M.C., Dhadda, S., Sethuraman, G., Kramer, L.D., Swanson, C.J., Li, D., Krause, S., Rissman, R.A., Walter, S., Raman, R., Johnson, K.A., Aisen, P.S., 2023. The AHEAD 3-45 Study: Design of a prevention trial for Alzheimer's disease. *Alzheimers Dement.* 19, 1227–1233. <https://doi.org/10.1002/alz.12748>.
- Reuter, M., Schmansky, N.J., Rosas, H.D., Fischl, B., 2012. Within-subject template estimation for unbiased longitudinal image analysis. *Neuroimage* 61, 1402–1418. <https://doi.org/10.1016/j.neuroimage.2012.02.084>.
- Risacher, S.L., Anderson, W.H., Charlil, A., Castelluccio, P.F., Shcherbinin, S., Saykin, A.J., Schwarz, A.J., 2017. Alzheimer's Disease Neuroimaging Initiative, Alzheimer disease brain atrophy subtypes are associated with cognition and rate of decline. *Neurology* 89, 2176–2186. <https://doi.org/10.1212/WNL.0000000000004670>.
- Salvadó, G., Molinuevo, J.L., Brugulat-Serrat, A., Falcon, C., Grau-Rivera, O., Suárez-Calvet, M., Pavia, J., Níñerola-Baízán, A., Perissinoti, A., Lomeña, F., Minguillon, C., Fauria, K., Zetterberg, H., Blennow, K., Gispert, J.D., Alzheimer's Disease Neuroimaging Initiative, for the ALFA Study, 2019. Centiloid cut-off values for optimal agreement between PET and CSF core AD biomarkers. *Alzheimers Res. Ther.* 11, 27. <https://doi.org/10.1186/s13195-019-0478-z>.
- Salvadó, G., Ossenkoppele, R., Ashton, N.J., Beach, T.G., Serrano, G.E., Reiman, E.M., Zetterberg, H., Mattsson-Carlsgren, N., Janelidze, S., Blennow, K., Hansson, O., 2023. Specific associations between plasma biomarkers and postmortem amyloid plaque and tau tangle loads. *EMBO Mol. Med.* 15, e17123. <https://doi.org/10.1522/emmm.202217123>.
- Sauty, B., Durrleman, S., 2023. Impact of sex and APOE-e4 genotype on patterns of regional brain atrophy in Alzheimer's disease and healthy aging. *Front. Neurol.* 14, 1161527. <https://doi.org/10.3389/fneur.2023.1161527>.
- Schwarz, A.J., Sundell, K.L., Charlil, A., Case, M.G., Jaeger, R.K., Scott, D., Bracoud, L., Oh, J., Suh, J., Pontecorvo, M.J., Dickerson, B.C., Siemers, E.R., 2019. Magnetic resonance imaging measures of brain atrophy from the EXPEDITION3 trial in mild Alzheimer's disease. *Alzheimers Dement.* 5, 328–337. <https://doi.org/10.1016/j.jalz.2019.05.007>.
- Schwarz, C.G., Gunter, J.L., Wiste, H.J., Przybelski, S.A., Weigand, S.D., Ward, C.P., Senjem, M.L., Vemuri, P., Murray, M.E., Dickson, D.W., Parisi, J.E., Kantarci, K., Weiner, M.W., Petersen, R.C., Jack Jr, C.R., 2016. Alzheimer's Disease Neuroimaging Initiative, A large-scale comparison of cortical thickness and volume methods for measuring Alzheimer's disease severity. *NeuroImage Clin.* 11, 802–812. <https://doi.org/10.1016/j.nicl.2016.05.017>.
- Shah, M., Kurth, F., Luders, E., 2021. The impact of aging on the subregions of the fusiform gyrus in healthy older adults. *J. Neurosci. Res.* 99, 263–270. <https://doi.org/10.1002/jnr.24586>.
- M. Shekari D. Vállez García L.E. Collij D. Altomare F. Heeman H. Pemberton N. Roé Vellvé S. Bullich C. Buckley A. Stephens G. Farrar G. Frisoni W.E. Klunk F. Barkhof J. D. Gispert ADNI and the AMYPAD consortium, Stress testing the Centiloid: Precision and variability of PET quantification of amyloid pathology 2024 Dement Alzheimers 10.1002/alz.13883.

- Skillbäck, T., Rosén, C., Asztely, F., Mattsson, N., Blennow, K., Zetterberg, H., 2014. Diagnostic performance of cerebrospinal fluid total tau and phosphorylated tau in Creutzfeldt-Jakob disease: results from the Swedish Mortality Registry. *JAMA Neurol.* 71, 476–483. <https://doi.org/10.1001/jamaneurol.2013.6455>.
- Tai, L.M., Thomas, R., Marottoli, F.M., Koster, K.P., Kanekyo, T., Morris, A.W.J., Bu, G., 2016. The role of APOE in cerebrovascular dysfunction. *Acta Neuropathol.* 131, 709–723. <https://doi.org/10.1007/s00401-016-1547-z>.
- Tosun, D., Schuff, N., Mathis, C.A., Jagust, W., Weiner, M.W., 2011. Alzheimer's Disease NeuroImaging Initiative, Spatial patterns of brain amyloid-beta burden and atrophy rate associations in mild cognitive impairment. *Brain* 134, 1077–1088. <https://doi.org/10.1093/brain/awv112>.
- Vahermaa, V., Aydogan, D.B., Raji, T., Armio, R.-L., Laurikainen, H., Saramäki, J., Suvisaari, J., 2023. FreeSurfer 7 quality control: Key problem areas and importance of manual corrections. *Neuroimage* 279, 120306. <https://doi.org/10.1016/j.neuroimage.2023.120306>.
- Villeneuve, S., Rabinovici, G.D., Cohn-Sheehy, B.I., Madison, C., Ayakta, N., Ghosh, P.M., La Joie, R., Arthur-Bentil, S.K., Vogel, J.W., Marks, S.M., Lehmann, M., Rosen, H.J.,
- Reed, B., Olichney, J., Boxer, A.L., Miller, B.L., Borys, E., Jin, L.-W., Huang, E.J., Grinberg, L.T., DeCarli, C., Seeley, W.W., Jagust, W., 2015. Existing Pittsburgh Compound-B positron emission tomography thresholds are too high: statistical and pathological evaluation. *Brain* 138, 2020–2033. <https://doi.org/10.1093/brain/awv112>.
- Wisch, J.K., Meeker, K.L., Gordon, B.A., Flores, S., Dincer, A., Grant, E.A., Benzinger, T.L., Morris, J.C., Ances, B.M., 2021. Sex-related differences in Tau Positron Emission Tomography (PET) and the Effects of Hormone Therapy (HT). *Alzheimer Dis. Assoc. Disord.* 35, 164–168. <https://doi.org/10.1097/WAD.0000000000000393>.
- Wolz, R., Aljabar, P., Hajnal, J.V., Hammers, A., Rueckert, D., 2010. Alzheimer's Disease NeuroImaging Initiative, LEAP: learning embeddings for atlas propagation. *Neuroimage* 49, 1316–1325. <https://doi.org/10.1016/j.neuroimage.2009.09.069>.
- Zilioli, A., Pancaldi, B., Baumeister, H., Busi, G., Misirocchi, F., Mutti, C., Florindo, I., Morelli, N., Mohanty, R., Berron, D., Westman, E., Spallazzi, M., 2025. Unveiling the hippocampal subfield changes across the Alzheimer's disease continuum: a systematic review of neuroimaging studies. *Brain Imaging Behav.* 19, 253–267. <https://doi.org/10.1007/s11682-024-00952-0>.